K^+ Currents Activated by Depolarization in Cardiac Fibroblasts

Yoshiyuki Shibukawa,* E. Lisa Chilton,* K. Andrew MacCannell,* Robert B. Clark,* and Wayne R. Giles*†

*Department of Physiology and Biophysics, Faculty of Medicine, University of Calgary, Calgary, Alberta, Canada; and †Department of Bioengineering, Whitaker Institute of Biomedical Engineering, University of California, San Diego, La Jolla, California

ABSTRACT K^+ currents expressed in freshly dispersed rat ventricular fibroblasts have been studied using whole-cell patch-clamp recordings. Depolarizing voltage steps from a holding potential of −90 mV activated time- and voltage-dependent outward currents at membrane potentials positive to ~−30 mV. The relatively slow activation kinetics exhibited strong dependence on the membrane potential. Selected changes in extracellular K^+ concentration ($[K^+]_o$) revealed that the reversal potentials of the tail currents changed as expected for a K^+ equilibrium potential. The activation and inactivation kinetics of this K^+ current, as well as its recovery from inactivation, were well-fitted by single exponential functions. The steady-state inactivation was well described by a Boltzmann function with a half-maximal inactivation potential ($V_{0.5}$) of −24 mV. Increasing $[K^+]_o$ (from 5 to 100 mM) shifted this $V_{0.5}$ in the hyperpolarizing direction by −11 mV. Inactivation was slowed by increasing $[K^+]_o$ to 100 mM, and the rate of recovery from inactivation was decreased after increasing $[K^+]_o$. Block of this K^+ current by extracellular tetraethylammonium also slowed inactivation. These $[K^+]_o$-induced changes and tetraethylammonium effects suggest an important role for a C-type inactivation mechanism. This K^+ current was sensitive to dendrotoxin-I (100 nM) and rTityustoxin Kα (50 nM).

INTRODUCTION

Fibroblasts are the most numerous cell types within mammalian hearts (Eghbali et al., 1988; Shiraishi et al., 1992; Goldsmith et al., 2004). They play an important role in producing and maintaining the extracellular matrix during both cardiac development and remodeling (Villarreal and Kim, 1998). Excessive deposition of fibrillar collagen in ventricles accompanies chronic heart failure, and is observed consistently after myocardial infarction during the acute phase (D'Armiento, 2002). It has been reported that contraction of atrial myocytes can induce slow changes in the membrane potential of atrial fibroblasts. These so-called mechanically induced potentials (Kohl et al., 1994) are thought to be modulated by mechanosensitive cation channels in atrial fibroblasts (Kamkin et al., 2003).

Recent studies in our laboratory suggest that K^+ conductances can regulate the membrane potential of ventricular fibroblasts and myofibroblasts from rat hearts (Chilton et al., 2003a,b). In both freshly isolated fibroblasts and myofibroblasts, the resting potential is modulated by inwardly rectifying K^+ current(s) and voltage-gated outward K^+ currents are expressed. Marked changes in the densities and/or the properties of K^+ currents may occur during normal cardiac development, as well as in conjunction with myocardial damage or disease (Nerbonne, 1998). There is also considerable interest in understanding the properties of voltage-dependent K^+ channels in cardiac fibroblasts, because fibroblasts may represent a novel target for the treatment of chronic heart failure (Long and Brown, 2002). This study was done to determine the biophysical properties of time- and voltage-dependent outward K^+ current(s) that are activated by voltage-clamp depolarizations in ventricular fibroblasts.

Time- and voltage-dependent K^+ conductances generate significant outward currents in most excitable cells (Coetzee et al., 1999; cf. Hille, 2001). Individual members of voltage-gated potassium (Kv) channel families can be identified on the basis of differences in voltage and time dependence of activation and inactivation, their pharmacological profiles, and/or molecular markers. For example, when expressed as homotetramer, Shaker-related Kv channels have ''delayed rectifier'' properties (Kv1.1, Kv1.2, Kv1.3, Kv1.5, and Kv1.6) and also may exhibit relatively rapid inactivation (Kv1.4, and Kv1.7).

Two distinct mechanisms of inactivation of Kv currents have been identified, and their molecular mechanisms have been studied in detail. Rapid ''N-type'' inactivation is produced by the N-terminus of a single α-subunit acting as a tethered blocking particle that binds to the internal pore of the channel (Hoshi et al., 1990; Zagotta et al., 1990). Slower ''C-type'' inactivation appears to involve all four subunits. Cooperative conformational changes are thought to occlude the external (outer) mouth of the pore of the channel (Choi et al., 1991; Hoshi et al., 1991). The development of, and recovery from, C-type inactivation are both much slower than those for N-type inactivation (Hoshi et al., 1991; Lopez-Barneo et al., 1993). N- and C-type inactivation, as well as recovery from their inactivation are modulated by elevation of the extracellular K^+ concentration $[K^+]_o$, and by external or internal application of tetraethylammonium (see Rasmusson et al., 1998; Fedida and Hesketh, 2001).

Submitted October 18, 2004, and accepted for publication February 23, 2005.

Address reprint requests to Dr. Wayne R. Giles, Dept. of Bioengineering, Whitaker Institute of Biomedical Engineering, University of California, San Diego, La Jolla, CA 92093-0412. Tel.: 858-822-4424; Fax: 858-534-4535; E-mail: wgiles@bioeng.ucsd.edu.

0006-3495/05/06/3924/12 $2.00

doi: 10.1529/biophysj.104.054429

Our experiments have identified the main biophysical properties which govern the time- and voltage-dependent K^+ currents activated by depolarization in freshly dissociated adult rat ventricular fibroblasts. The whole-cell patch-clamp method was utilized to study activation and inactivation kinetics, and determine steady-state properties of these K^+ current(s). Additional studies demonstrated a dependence of these parameters on changes in $[K^+]_o$, and provided preliminary descriptors of the pharmacological profile of these K^+ currents. In combination, our results are consistent with the conclusion that a Kv channel subtype (e.g., Kv1.2 or Kv 1.6) that exhibits C-type inactivation is expressed in fibroblasts from the ventricles of adult rats.

MATERIALS AND METHODS

Enzymatic dissociation of rat ventricular fibroblasts

Fibroblasts were obtained by enzymatic dispersion from ventricles of male Sprague-Dawley rats (200–250 g). All animals were treated in accordance with the Guiding Principles for the Care and Use of Animals in the Field of Physiological Sciences, which have been approved by the Council of the American Physiological Society. In brief, each heart was removed after a thoracotomy under surgical anesthesia with isoflurane (3–5%). The anesthesia was maintained at surgical plane (indicated by the lack of a toe pinch reflex) with methoxyflurane during the surgery. The dissected heart was perfused (at a flow rate of 8 ml/min) at 37°C using a Langendorff apparatus connected to a peristaltic pump. Initially, Tyrode's solution containing 1 mM Ca^{2+} was applied (5 min); this was followed by Ca^{2+}-free Tyrode's solution (5 min). For initial enzymatic digestion, the heart was perfused with Tyrode's solution (with 40 μM Ca^{2+}) containing 0.004% collagenase (Type II, Worthington, Lakewood, NJ) and 0.0004% protease (type XIV) at 37°C for 12 min. For the final stage of enzymatic digestion, the ventricles were removed from the heart, and digested by cutting them into small segments and then shaking in a solution (100 μM Ca^{2+}) containing 0.1% collagenase type II, 0.01% protease type XIV, and 0.5% bovine serum albumin at 37°C for 20–60 min. The resulting suspension of isolated fibroblasts was diluted and stored at room temperature (21 ± 1.0°C) for 60 min in a buffer (''KB'' buffer) to halt enzymatic digestion. Single cardiac fibroblasts were used for electrophysiological recordings within 6 h after dissociation.

Fibroblasts were allowed to settle on the glass bottom of a recording chamber (0.5 ml in volume) that was placed on the stage of an inverted microscope (Axiovert 25, Zeiss, Jena, Germany), and were viewed under phase-contrast optics. Control recording solutions and those containing blocking agents were applied by superfusion using a rapid gravity-fed perfusion system (ALA Scientific Instruments, Westbury, NY).

Solutions and reagents

During the cell dispersion steps, the Tyrode's solution had the following composition (in mM): 140 NaCl, 5.4 KCl, 1 $CaCl_2$, 1 $MgCl_2$, 1 Na_2HPO_4, 5 HEPES, and 10 glucose (pH 7.4 with NaOH). $CaCl_2$ concentration was adjusted to be Ca^{2+}-free, 40 μM, or 1 mM during timed Langendorff perfusions, and was adjusted to 100 μM during final cell dispersion, step as indicated. To terminate each enzymatic digestion, a ''KB'' buffer was applied. It contained (in mM) 100 potassium glutamate, 10 potassium aspartate, 25 KCl, 10 KH_2PO_4, 2 $MgSO_4$, 20 taurine, 5 creatine, 0.5 EGTA, 20 glucose, 5 HEPES, and 1% bovine serum albumin (pH 7.2 with KOH).

During whole-cell patch-clamp recordings, the extracellular solution consisted of (in mM) 140 NaCl, 5.4 KCl, 1 $CaCl_2$, 1 $MgCl_2$, 10 HEPES, 5.5 glucose, and 7.14 mannitol. In the experiments in which extracellular K^+ concentration ($[K^+]_o$) was changed, $[K^+]_o$ was altered by isoosmotic substitution of KCl for NaCl. When tetraethylammonium chloride (TEA) was used, it was substituted for NaCl. As a part of a preliminary pharmacological characterization of Kv currents the pharmacological agents dendrotoxin-I (DTX-I; Alomone Laboratories, Jerusalem, Israel) and rTityustoxin Kα (rTTSX-Kα; Alomone Laboratories) were applied. Stock solutions of these agents were prepared in distilled water, and diluted with extracellular solution to the appropriate concentration immediately before use. The pipette-filling solution contained (in mM) 110 potassium aspartate, 20 KCl, 12 NaCl, 1 $CaCl_2$, 10 EGTA, 4 K_2ATP, 1 $MgCl_2$, and 10 HEPES. The pH was adjusted to 7.2 for intracellular solution with KOH and 7.4 for extracellular solutions with NaOH. Most reagents were obtained from Sigma Chemical (St. Louis, MO).

Data acquisition and analysis: whole-cell recording techniques

The conventional whole-cell voltage clamp recording method was employed. Patch pipettes with resistances of 3–7 MΩ were pulled from capillary tubes using a Flaming/Brown micropipette puller (Model P87/PC, Sutter Instrument, Novato, CA), and then back-filled with the intracellular solution. Whole-cell currents were measured using a patch-clamp amplifier (L/M-EPC-7, List-Medical, Darmstadt, Germany) that allowed for compensation of cell capacitance and series resistance. The currents were monitored and stored after digitizing the analog signals at 10 kHz (DigiData 1200, Axon Instruments, Foster City, CA) using pCLAMP software (Axon Instruments). Current records were filtered at 3 kHz. Voltage commands were generated by a software-driven digital-to-analog converter (DigiData 1200). Data were analyzed off-line using pCLAMP, and a technical graphics/analysis program (ORIGIN, MicroCal Software, Northampton, MA). All experiments were conducted at room temperature (21 ± 1.0°C).

The membrane capacitance of fibroblast was calculated from the capacitative transient evoked by 10 mV depolarizing steps from a holding potential (V_h) of −90 mV. Current amplitudes were normalized to these single cell capacitance values and expressed as current densities. A correction of −10 mV was applied for liquid junction potentials (Barry, 1994).

The voltage dependence of steady-state inactivation of these K^+ currents was obtained by fitting the data with a Boltzmann function:

$$I/I_{max} = 1/\{1 + \exp[(V_h - V_{0.5})/k]\}, \quad (1)$$

where V_h is the holding potential, $V_{0.5}$ is the membrane potential at which the peak current is inactivated by 50%, and k is the slope factor.

The kinetics of activation and inactivation, as well as the recovery time course were obtained by fitting experimental data with single exponential functions using Origin software. Analysis of a large number of current traces from isolated fibroblasts from rat ventricular tissue studies over an 18-month period consistently showed that a single exponential function provided a suitable fit to the time courses of both inactivation of the current onset and deactivation of the corresponding tail currents.

Statistics

The results are expressed as mean ± SE of n observations, where n represents the number of fibroblast cells studied. Student's t-tests were used to evaluate statistical significance. Values of $P < 0.05$ were considered significant.

RESULTS

Passive membrane properties of acutely isolated cardiac fibroblasts

Freshly dissociated ventricular fibroblasts are approximately spherical, with a diameter of ~8 μm. They have no

cross-striations which are characteristic of adult ventricular myocytes (cf. Chilton et al., 2005). In addition, the fibroblasts chosen for this study could be identified based on distinct immunoreactivity. They exhibited vimentin-positive and smooth-muscle actin-negative staining (not shown). These findings indicate that these cells are cardiac fibroblasts, not endothelial cells or myofibroblasts (Villarreal et al., 1993; Suh et al., 1999; Tomasek et al., 2002; Chilton et al., 2005). In our initial experiments, the resting membrane potential (E_m) was measured immediately after the establishment of a gigaohm seal using a conventional whole-cell recording configuration. E_m averaged -58.0 ± 3.9 mV ($n = 13$) in 5 mM $[K^+]_o$. These isolated cardiac fibroblasts had a membrane capacitance of 4.5 ± 0.4 pF and an input resistance of 5.5 ± 0.6 GΩ ($n = 37$); ~90% of these freshly isolated cardiac fibroblasts expressed the pattern of time- and voltage-dependent outward K^+ currents shown in Fig. 1.

Time- and voltage-dependent outward currents in cardiac fibroblasts

The time- and voltage-dependent transmembrane currents in cardiac fibroblasts were investigated under voltage-clamp conditions using conventional whole-cell patch-clamp recordings. The current records in Fig. 1 *A* were elicited by 400-ms voltage clamp steps (*upper traces*) ranging from −110 to +50 mV. Clamp steps were applied in 10 mV increments from a holding potential (V_h) of −90 mV in the presence of either 10 mM (*middle traces*) and 100 mM $[K^+]_o$ (*lower traces*). In the membrane potential range from ~0 to +50 mV, the outward currents exhibited slow activation and no apparent inactivation during 400-ms depolarizations (Fig. 1 *A*). Current-voltage (I/V) relationships were obtained by plotting the steady-state amplitude of these currents against membrane potential. Small differences in fibroblast size were accounted for by normalizing for the measured capacitance and expressing current amplitudes in terms of current densities (pA/pF). Fig. 1 *B* shows I/V relationships obtained at four different extracellular K^+ concentrations. Note that the activation threshold for the outward current was ~−30 mV in 5 mM $[K^+]_o$; and that at more depolarized membrane voltages, the I/V relationship is approximately linear. In contrast, in 100 mM $[K^+]_o$, relatively large inwardly directed currents developed at membrane potentials between −40 and 0 mV. This result suggests that these currents activate near −40 mV under these conditions. This shift of the threshold for activation (~−10 mV) of outward current in high (100 mM) $[K^+]_o$ can be seen clearly in the I/V relationships.

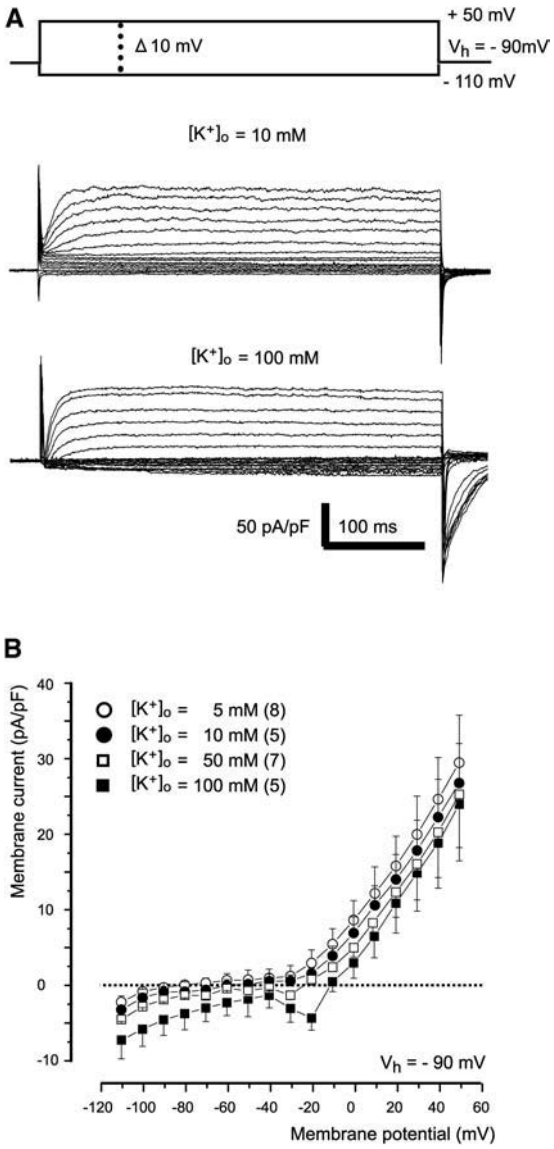

FIGURE 1 Time- and voltage-dependent outward currents in enzymatically isolated rat ventricular fibroblasts. (*A*) Outward currents were elicited by 400-ms voltage steps (*upper traces*) from a holding potential, V_h, of −90 mV to membrane potentials between −110 to +50 mV. Clamp steps were applied at 0.1 Hz. Typical experimental results in both 10 mM (*middle traces*) and 100 mM $[K^+]_o$ (*lower traces*) are shown. (*B*) The I/V relationships denote the steady-state current changes in 5 (○), 10 (●), 50 (□), and 100 mM (■) $[K^+]_o$ as indicated in the inset. The voltage clamp protocol was the same as in *A*. Each point indicates the mean ± SE of data from several experiments (indicated by the numbers in parentheses in the *inset*).

K^+ selectivity of transmembrane currents in ventricular fibroblasts

To investigate the ion selectivity of these time- and voltage-dependent outward currents, a tail current analysis was carried out. In these studies, the reversal potentials were measured in four different $[K^+]_o$: 5, 10, 50, and 100 mM. In each experiment, families of tail currents were elicited by stepping the membrane potential from the V_h (−90 mV) to +50 mV before hyperpolarizing in 10-mV increments into a membrane potential range between −110 and −10 mV. Fig. 2 *A* shows typical tail currents recorded in 5 mM $[K^+]_o$ (*middle traces*) and 100 mM $[K^+]_o$ (*lower traces*). When the tail current amplitudes (measured 20 ms after the start of

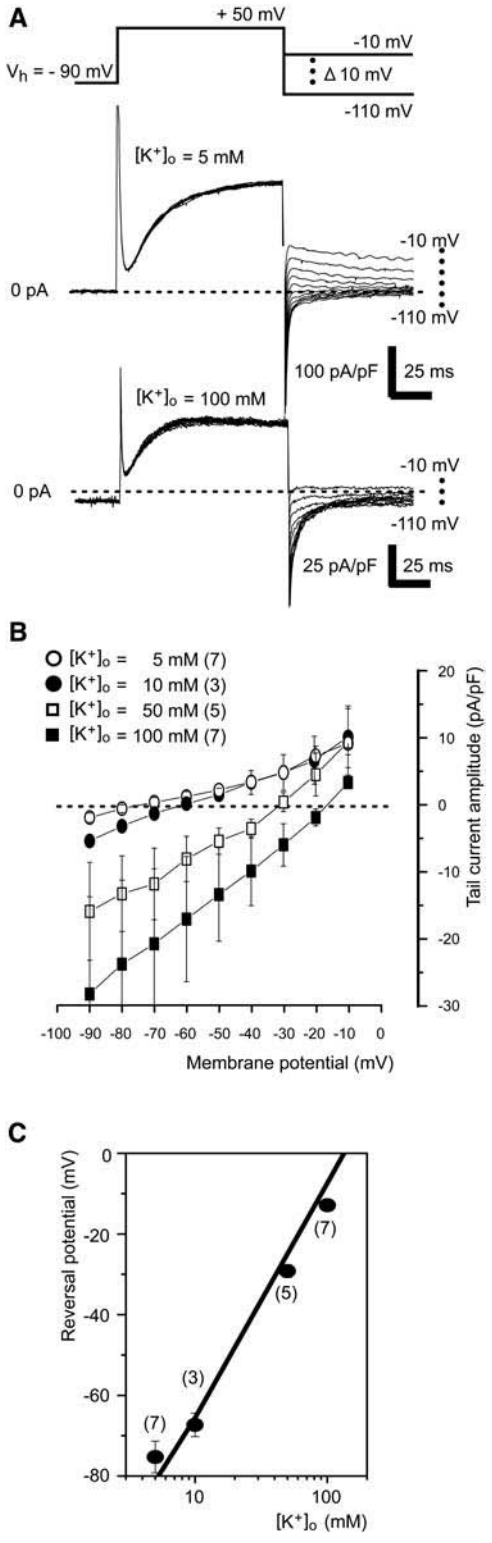

FIGURE 2 Tail current analysis of cardiac fibroblast outward currents. (*A*) Typical examples of a family of tail currents obtained in response to a depolarization to +50 mV, followed by repolarization to the membrane potentials indicated. The voltage clamp protocol is shown in the top panel. These current records were obtained in 5 mM $[K^+]_o$ (*middle traces*) and 100 mM $[K^+]_o$ (*lower traces*). (*B*) I/V relationships obtained by plotting the tail current amplitudes for a given $[K^+]_o$ as indicated in the inset, for several experiments (numbers in parentheses). The voltage clamp protocol was the same as in *A*. Each point indicates the mean ± SE of data from several experiments. (*C*) Pooled data (mean ± SE) from several experiments (numbers in parentheses) show the measured reversal potentials plotted against $[K^+]_o$ (●) on a semilogarithmic scale. The slope predicted by the Nernst equation for an ideal K^+ conductance (59 mV per 10-fold change in $[K^+]_o$) is denoted by the solid line.

hyperpolarizing pulse to avoid current changes due to cell capacitance) were plotted as a function of applied membrane potential, reversal potentials were obtained (Fig. 2 *B*). The mean reversal potential values (Fig. 2 *B*) were −75 ± 4 mV in 5 mM $[K^+]_o$, −67 ± 3 mV in 10 mM $[K^+]_o$, −29 ± 2 mV in 50 mM $[K^+]_o$, and −13 ± 1 mV in 100 mM $[K^+]_o$ ($n = 4$–7 cells). Fig. 2 *C* shows a semilog plot of these reversal potentials, against $[K^+]_o$. The mean values for reversal potentials with 5–100 mM $[K^+]_o$ closely approximated those expected for a K^+ selective current (Fig. 2 *C*, *solid line*), assuming $[K^+]_i$ to be 140 mM (see Materials and Methods).

Envelope of tails test assessment of ventricular fibroblast K^+ currents

To assess the hypothesis that the time- and voltage-dependent K^+ current changes in cardiac fibroblasts arise from a single K^+ conductance, an envelope of tails test (Noble and Tsien, 1969) was conducted. Cardiac fibroblasts were depolarized from a holding potential of −90 mV to +40 mV for various durations, ranging from 10 to 100 ms (Fig. 3 *A*, *upper trace*). The envelope of tail currents (I_{tail}) elicited immediately upon repolarization to a membrane potential of 0 mV was compared with the magnitude of the outward current (I_{pulse}) which was activated during depolarization for each depolarizing pulse duration.

In a classical Hodgkin-Huxley scheme, if the time and voltage dependence of the K^+ current change in cardiac fibroblasts is controlled by a single gating mechanism, then the time course of envelope of the current tails at any fixed potential is expected to closely match the time course of the current activation itself (Hodgkin and Huxley, 1952). In addition, if time- and voltage-dependent K^+ current in cardiac fibroblasts results from a single conductance component, the ratio of I_{tail} to I_{pulse} for a given depolarizing pulse is expected to be constant, regardless of the pulse duration (Sanguinetti and Jurkiewicz, 1990).

Fig. 3 *A* (*lower traces*) shows a series of current traces that comprised a representative envelope of tails test. In this figure, current records elicited by progressively larger steps (from 10 to 100 ms) are shown, together with respective tail currents. In 5 mM $[K^+]_o$, as expected, the activating current (I_{pulse}) was larger than the I_{tail} at all clamp pulse durations, and the amplitudes of both I_{tail} and I_{pulse} progressively increased with increasing duration of depolarizations. In Fig. 3 *B*, the averaged amplitudes for both I_{tail} and I_{pulse} are plotted against the clamp pulse durations. These records

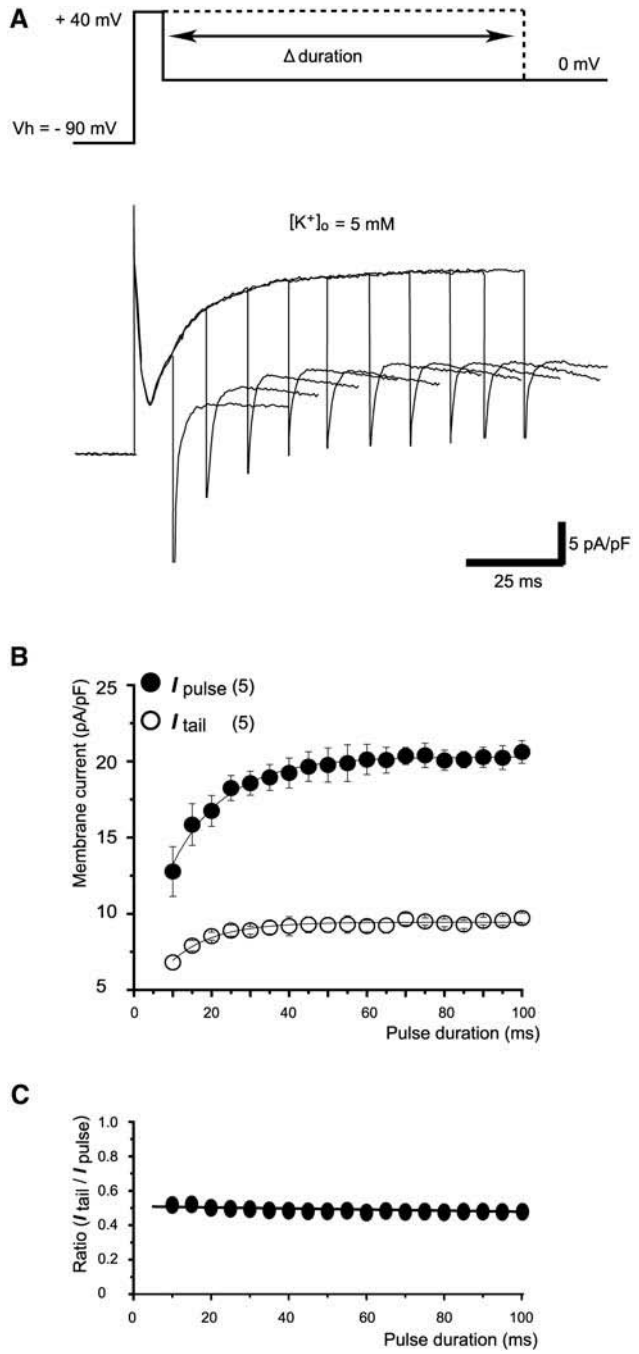

FIGURE 3 Envelope of tails test in cardiac fibroblasts. (*A*) Representative family of K^+ current changes (*middle traces*) recorded in response to rectangular voltage clamp depolarizations to +40 mV having durations ranging from 10 to 100 ms, in 10-ms steps, in 5 mM $[K^+]_o$. Each depolarizing step was followed by repolarization to 0 mV, at which all tail currents were recorded. The voltage clamp protocol is shown in the *top panel*. (*B*) The mean current amplitudes for the amplitude of the tail current (I_{tail}; ○) elicited upon repolarization, and the magnitude of the outward current (I_{pulse}; ●) activated during depolarization are plotted as a function of depolarizing pulse duration (in 5-ms steps). Each data point indicates the mean ± SE for five experiments. (*C*) The ratio I_{tail} to I_{pulse} (I_{tail}/I_{pulse}) as a function of depolarizing pulse duration. Each data point indicates the mean ± SE for five experiments.

were all well-fitted by a single exponential function. This analysis yielded a mean time constant of 19.9 ± 3.1 ms for I_{pulse} ($n = 5$) and 19.7 ± 3.8 ms for I_{tail} ($n = 5$). There were no significant differences between time courses of I_{tail} and I_{pulse} ($P > 0.1$). In addition, the time constants for each tail current deactivation were also well-fitted by a single exponential function, i.e., the deactivation time course remained the same regardless of clamp pulse duration, with a mean time constant of 32.5 ± 2.5 ms for 10 ms ($n = 5$) and 32.3 ± 0.9 ms ($n = 5$) for 100 ms of pulse durations. Note also that the ratio of I_{tail} to I_{pulse} (I_{tail}/I_{pulse}) was constant (0.51) regardless of the duration of the depolarizing pulse (Fig. 3 *C*). In combination, these findings strongly suggest that time- and voltage-dependent K^+ current in cardiac fibroblasts arises from a single K^+ conductance. Although it is theoretically possible that, e.g., two interacting transmembrane currents with very different reversal potentials could interact to produce this pattern of results, in our experience with similar types of analysis on 12 different types of cardiac myocytes or intracardiac neurons, this is extremely unlikely. We acknowledge that unless this analysis could, in principle, be confounded by restricted extracellular diffusion, which may cause $[K^+]_o$ accumulation (Attwell et al., 1979; Yasui et al., 1993).

Steady-state inactivation of cardiac fibroblast K^+ currents

The voltage dependence of steady-state inactivation of this outward K^+ current was studied in four different $[K^+]_o$. Fig. 4 *A* illustrates a family of currents (Fig. 4 *A*, *lower traces*) obtained by stepping to a membrane potential of +50 mV from a V_h, which varied from −90 to +10 mV (Fig. 4 *A*, *upper traces*) in 5 mM $[K^+]_o$. In each recording, V_h was maintained for at least 30 s before applying the depolarizing step. As expected, the outward current amplitude decreased as the holding potential became more depolarized. In Fig. 4 *B*, current sizes for a given holding potential (*I*) have been normalized to the amplitude at a holding potential of −90 mV (I_{max}) and then plotted against the selected holding potential value. This type of data was obtained in 5 (*open circles*), 10 (*solid circles*), 50 (*open squares*), and 100 mM (*solid squares*) $[K^+]_o$. As shown in Fig. 4 *B*, each set of these data points was well-fitted with a Boltzmann function (Eq. 1). The semilog plot of the $V_{0.5}$ against $[K^+]_o$ (Fig. 4 *C*) shows that the values of $V_{0.5}$ were shifted in the hyperpolarizing direction by increasing $[K^+]_o$. The best fits of $V_{0.5}$ were −24.3 ± 1.1 mV in 5 mM, −31.3 ± 2.1 mV in 10 mM, −35.0 ± 3.0 mV in 50 mM, and −35.5 ± 3.0 mV in 100 mM $[K^+]_o$ ($n = 4$–7 cells). The values of k were 7.0 ± 0.9 mV/e-fold change in membrane potential in 5 mM, 8.9 ± 1.3 mV/e-fold change in 10 mM, 6.9 ± 0.6 mV/e-fold change in 50 mM, and 8.1 ± 0.8 mV/e-fold change in 100 mM $[K^+]_o$ ($n = 4$–7 cells). Note that the value of $V_{0.5}$ in 5 mM $[K^+]_o$ was significantly different from each $V_{0.5}$ in 10 mM ($P <$

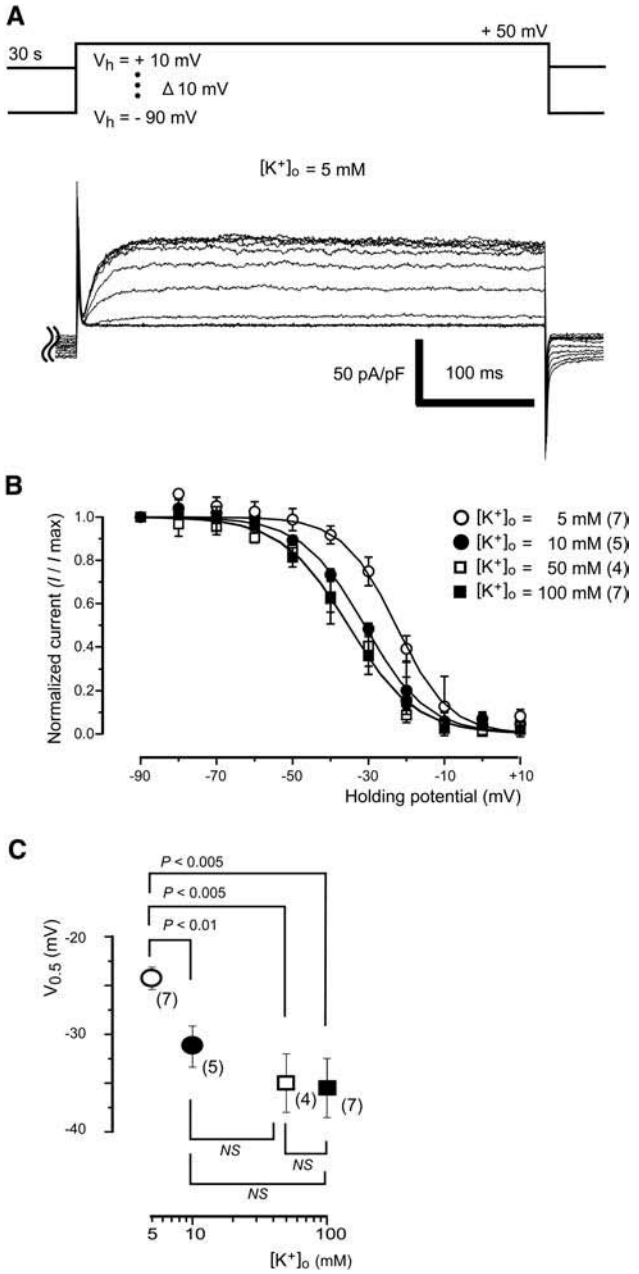

FIGURE 4 Steady-state inactivation of K^+ current. (*A*) Family of currents obtained by stepping to the membrane potential of +50 mV from a series of holding potentials (−90 to +10 mV) in 5 mM $[K^+]_o$. Top panel shows the voltage clamp protocol. In each recording, the holding potential, V_h, was maintained for at least 30 s before the depolarizing step was applied. Note that the amplitude of the outward current declines as the holding potential is made more positive. (*B*) Steady-state inactivation curve obtained by plotting steady-state outward current as a fraction of outward current at −90 mV (I/I_{max}) versus holding potential in four different $[K^+]_o$ (as indicated in the *inset*). Each point denotes the mean ± SE for several experiments (numbers in parentheses in the *inset*). Each of these data sets was fitted with a Boltzmann equation (Eq. 1; see text). (*C*) Pooled data (mean ± SE) from several experiments (numbers in parentheses), including estimated $V_{0.5}$ plotted against $[K^+]_o$ on a semilogarithmic scale. Statistically significant differences between $V_{0.5}$ measurements are indicated as *P*-values, whereas a lack of significant difference between them is indicated as *NS*.

0.01), 50 mM ($P < 0.005$), as well as 100 mM ($P < 0.005$) $[K^+]_o$. However, there were no significant differences between the values of k amongst these different $[K^+]_o$.

Activation kinetics of K^+ currents in cardiac fibroblasts

Fig. 5 *A* shows examples of fibroblast K^+ current activation in response to voltage clamp depolarizations ranging between +10 and +50 mV from V_h of −90 mV in 10 mM $[K^+]_o$ (*gray lines*). The heavy lines in Fig. 5 *A* denote single exponential functions that provided each best fit. The mean values of these time constants (τ) of activation versus membrane potential from +10 mV to +50 mV are shown in

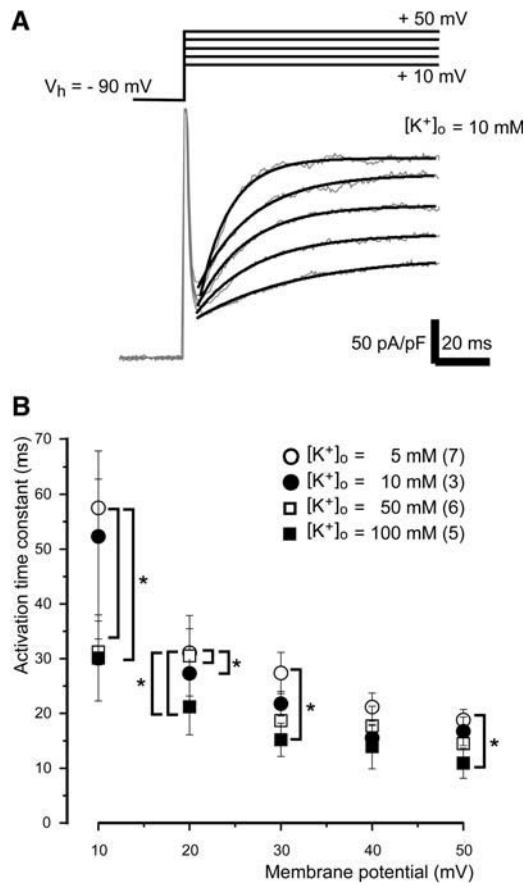

FIGURE 5 Activation kinetics of fibroblast K^+ current. (*A*) Family of the outward currents recorded at membrane potentials between +10 and +50 mV from a V_h of −90 mV (*gray lines*) with 10 mM $[K^+]_o$. The superimposed heavy lines denote the best fit of a single exponential function. This analysis yielded activation time constants (τ) ranging from 45 ms at a membrane potential of +10 mV to 17 ms at a membrane potential of +50 mV. (*B*) The mean values of these time constants (τ) of activation versus membrane potentials from +10 mV to +50 mV in four different $[K^+]_o$ were obtained, as indicated in the inset. Each point denotes the mean ± SE for data from several experiments (numbers in parentheses in the *inset*). Statistically significant differences between these activation time constants at fixed membrane potentials in different $[K^+]_o$ are indicated by asterisks: $*P < 0.05$.

Fig. 5 *B*. These data were obtained in four different $[K^+]_o$. As expected, the time constants of activation exhibited strong dependence on the membrane potential, ranging from 57.5 ± 5.2 ms at +10 mV to 18.8 ± 1.9 ms at +50 mV in 5 mM $[K^+]_o$ ($n = 7$). In 100 mM $[K^+]_o$ the corresponding time constant values ranged from 30.1 ± 7.9 ms at +10 mV to 10.9 ± 2.7 ms at +50 mV ($n = 5$).

Inactivation kinetics of cardiac fibroblast K^+ current

Inactivation, which developed very slowly during depolarization, was studied by analyzing the current decay during long (5-s) voltage clamp steps. In these experiments, individual fibroblasts were depolarized from 0 mV to +50 mV from a V_h of −90 mV (Fig. 6 *A*, *upper trace*). In 5 mM $[K^+]_o$, the outward current during these long voltage steps (Fig. 6 *A*, *gray lines*) showed slow inactivation with a time course that was well-fitted by a single exponential function (Fig. 6 *A*, *heavy lines*). The mean values for time constants (τ) of inactivation in 5 mM and 100 mM $[K^+]_o$ were significantly different (Fig. 6 *B*). The inactivation time constants ranged from 3146.1 ± 564.1 ms at 0 mV to 1690.4 ± 106.2 ms at +50 mV in 5 mM $[K^+]_o$ ($n = 4$). As shown in Fig. 6 *B*, corresponding values ranged from 4268.9 ± 690.3 ms at 0 mV to 2783.1 ± 239.0 ms at +50 mV in 100 mM $[K^+]_o$ ($n = 4$).

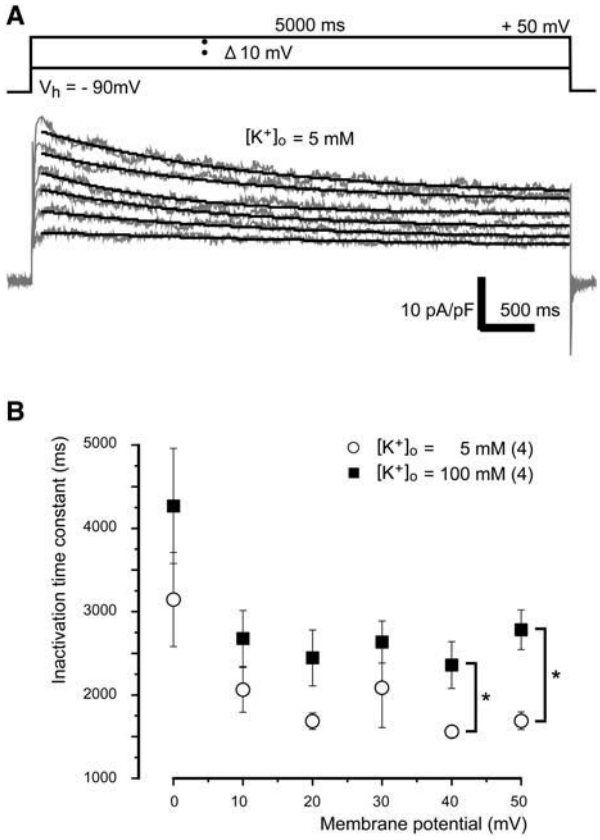

FIGURE 6 Inactivation kinetics of the cardiac fibroblast K^+ current. (*A*) An example of the outward currents obtained at selected membrane potentials between +10 and +50 mV from a V_h of −90 mV (*gray lines*) in 5 mM $[K^+]_o$. In this experiment, 5-s voltage clamp steps were applied, so that the slowly developing inactivation could be characterized. The superimposed heavy lines denote best fit of a single exponential function. This analysis yielded inactivation time constants (τ) ranging from 2461 ms at a membrane potential of +10 mV to 1894 ms at a membrane potential of +50 mV. (*B*) Mean values of the time constants (τ) of activation versus membrane potentials from 0 mV to +50 mV in 5 mM (○) and 100 mM (■) $[K^+]_o$ are shown. Each point indicates the mean ± SE of data from several experiments (numbers in parentheses in the *inset*). Statistically significant differences between these values of inactivation time constants are indicated by asterisks: $*P < 0.05$.

Recovery from inactivation of cardiac fibroblast K^+ current

To analyze the recovery or reactivation of these K^+ currents, a standard double-pulse voltage protocol was utilized (Fig. 7 *A*, *upper trace*). The magnitude and duration (5 s) of the first pulse (prepulse) were chosen so that K^+ currents activated and then fully inactivated. After a variable interpulse interval at −90 mV, a second depolarizing clamp pulse to +50 mV (60 ms in duration) was applied. The current elicited by this test pulse provides a measure of recovery from the inactivated state induced by the prepulse. The interval between each pair of clamp pulses was 30 s, which ensured that no inactivation accumulated between each P1-P2 protocol. Fig. 7 *A* shows representative raw data. The interpulse interval varied from 200 to 2,000 ms in increments of 200 ms. In both 5 mM $[K^+]_o$ (Fig. 7 *A*) and 100 mM $[K^+]_o$ (not shown), >50% of the current inactivated during the 5-s prepulse at +50 mV. For this reason, after a brief interval, peak current amplitudes recorded during test pulses (I_{peak2}) were much smaller than those of the first prepulse (I_{peak1}). I_{peak2} recovered progressively as the interpulse interval increased. The averaged fractional recovery in two different $[K^+]_o$ is plotted against the interpulse intervals (Fig. 7 *B*). The records were well-fitted by a single exponential function which yielded a mean time constant of 1051.0 ± 154.7 ms in 5 mM $[K^+]_o$ ($n = 4$) and 728.0 ± 69.8 ms in 100 mM $[K^+]_o$ ($n = 4$). The corresponding offset values were 0.86 ± 0.06 in 5 mM $[K^+]_o$ ($n = 4$) and 0.92 ± 0.02 in 100 mM $[K^+]_o$ ($n = 4$). These offsets need to be accounted for since the recovery from inactivation is not complete, even after an interpulse interval of 7 s. The bar graph in Fig. 7 *C* demonstrates that the mean time constant of recovery in 5 mM $[K^+]_o$ was significantly slower than that in 100 mM $[K^+]_o$ ($P < 0.05$).

Slow inactivation of fibroblast K^+ current exhibits C-type characteristics

To investigate further whether N- or C-type (or both) inactivation processes regulate the K^+ current in ventricular fibroblasts, the effect of superfusion of TEA in normal

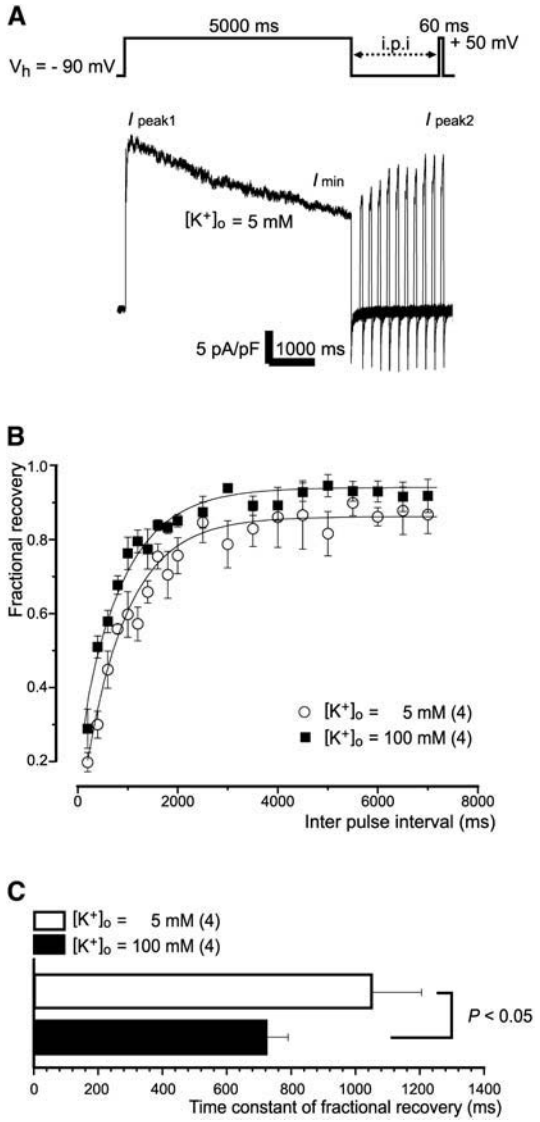

FIGURE 7 Recovery of K^+ current from slow inactivation. (*A*) Representative example of a family of currents activated from a V_h of −90 mV by a 5-s step to +50 mV (first pulse) in 5 mM $[K^+]_o$. The initial depolarization was followed by a second depolarizing clamp step to +50 mV (60 ms in duration). In this experiment, the interpulse interval (*i.p.i.*) was varied from 200 to 2000 ms, in increments of 200 ms. This double-pulse voltage protocol is illustrated in the top panel. The interval between each two-pulse protocol was 30 s. I_{peak1}, peak current amplitudes elicited by the first prepulse; I_{peak2}, peak current amplitudes elicited by the second (test) pulses; I_{min}, current amplitudes at 5 s of first prepulse. (*B*) The mean values of the fractional recovery (see text) versus interpulse interval from 200 to 7000 ms with 5 and 100 mM $[K^+]_o$ are shown in the inset. The fractional recovery was quantified using

$$Fractional\,Recovery = (I_{peak2} - I_{min})/(I_{peak1} - I_{min}).$$

Each point indicates the mean ± SE for four experiments. Individual recovery time constants were well-fitted by a single exponential function. (*C*) Summary bar graph. Note that the mean time constant of recovery in 5 mM $[K^+]_o$ was significantly slower than that in 100 mM $[K^+]_o$. Statistically significant differences are indicated as *P*-values.

Tyrode's solution on the inactivation kinetics was studied. It is known that blockade of K^+ channels by extracellular TEA is accompanied by a concomitant slowing of C-type inactivation; in contrast, rapid N-type inactivation is TEA-insensitive (Choi et al., 1991; Grissmer and Cahalan, 1989). Our results showed that in ventricular fibroblasts, changes in $[K^+]_o$ strongly modulate both the rate of inactivation and recovery from inactivation of the outward K^+ current (Figs. 6 and 7). These findings suggest that these K^+ currents exhibit C-type inactivation.

As shown in Fig. 8, application of extracellular TEA (30 mM) partially, but significantly blocked the outward currents elicited by long (40-s) voltage clamp pulses from a V_h of −90 mV and also slowed the rate of inactivation. The time constant (τ) of inactivation in 30 mM TEA was ~1.7 fold ($n = 3$) slower than that of inactivation in control (Fig. 8 *A*) at a membrane potential of +50 mV. To document this finding,

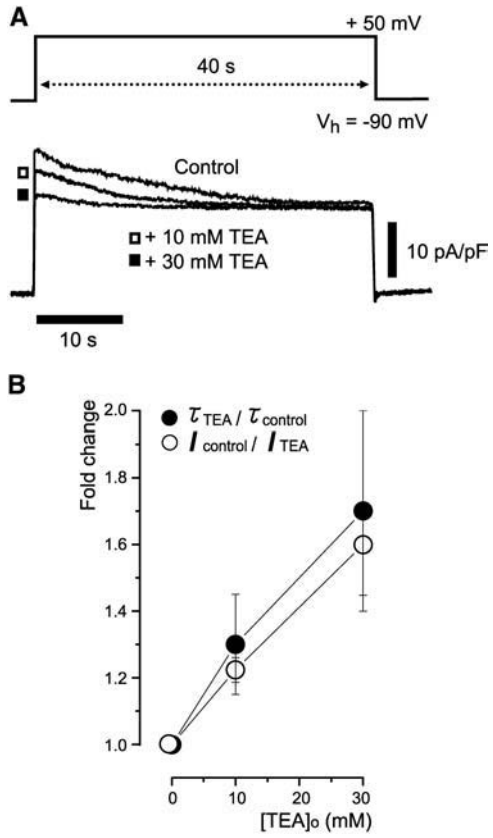

FIGURE 8 Effects of TEA blockade on inactivation kinetics of K^+ currents in ventricular fibroblasts. (*A*) Inactivation of K^+ current during prolonged voltage step (*40 s*) from V_h of −90 mV to +50 mV before (*Control*) and during application of extracellular TEA (30 mM). The voltage clamp protocol is shown in the top panel. (*B*) Effects of extracellular TEA on steady-state current (○), and slowing of inactivation (●). Both parameters are expressed as the fold change from control ($I_{control}/I_{TEA}$ or $\tau_{TEA}/\tau_{control}$). Inactivation time constants (τ) were measured by fitting an exponential decay function at a membrane potential of +50 mV. The voltage clamp protocol was the same as in *A*. Each point indicates the mean ± SE for each of three experiments.

we examined the concentration dependence of the effect of TEA on current amplitude and inactivation kinetics. In Fig. 8 *B*, both parameters are expressed in terms of fold changes from control (control current/current with TEA ($I_{control}/I_{TEA}$) or τ in TEA/τ in control ($\tau_{TEA}/\tau_{control}$), as a function of the selected extracellular TEA concentrations. Note that the time constant (τ) of inactivation increases by a factor similar to that by which the current amplitude is reduced. Thus, the degree of slowing of inactivation appears to be correlated with the extent of current blockade (Fig. 8 *B*), and both parameters show a dependence on the external TEA concentration within the range (10–30 mM). These results further suggest that outward currents in cardiac fibroblasts exhibit C-type inactivation (Choi et al., 1991; Grissmer and Cahalan, 1989).

Pharmacological properties of Kv channels expressed in cardiac fibroblasts

In the final set of experiments, a number of pharmacological agents that are used as K^+ channel blockers were applied in an attempt to identify the α-subunit responsible for these time- and voltage-dependent K^+ (Kv) channels. Initially, the effects of toxins, which are considered to be selective blockers of Kv family α-subunit, were examined. Outward currents were activated by 400 ms depolarizing voltage clamp steps to +50 mV from a V_h of −90 mV before, during, and after application of Kv channel toxins. As shown in Fig. 9, DTX-I and rTTSX-Kα (Werkman et al., 1993) partially blocked steady-state currents at +50 mV. Dendrotoxin (100 nM) resulted in a 15.7 ± 3.2% ($n = 3$, $P < 0.05$; Fig. 9, *upper traces*) decrease, and 50 nM rTTSX-Kα also significantly reduced steady-state currents by 20.0 ± 5.0% ($n = 3$, $P < 0.05$; Fig. 9, *upper traces*). In contrast, the steady-state outward K^+ currents in cardiac fibroblasts were unaffected by the application of 10 nM rTTSX-Kα (100.0 ± 2.0% ($n = 3$); Fig. 9, *lower traces*). The pattern of results suggests that cardiac fibroblasts express K^+ currents due to the Kv family, perhaps Kv 1.2 or Kv 1.6 (see Discussion).

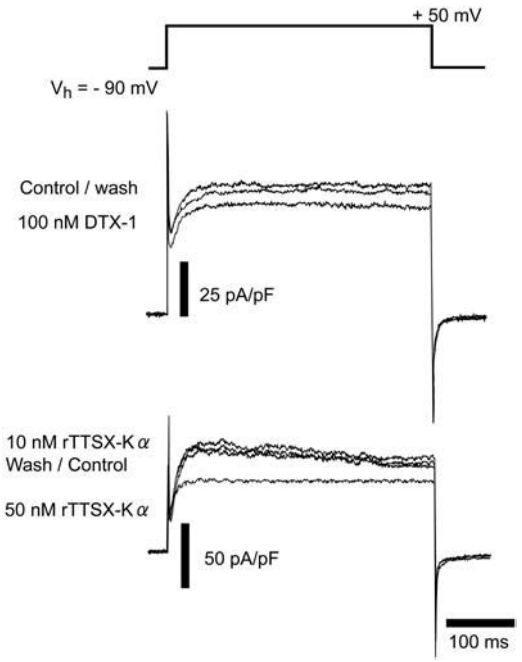

FIGURE 9 Toxin-induced inhibition of ventricular fibroblast K^+ currents. Outward currents were activated by a 400-ms depolarizing voltage step to +50 mV from a V_h of −90 mV (*top panel*) before (*Control*), during, and after (*Wash*) application of Kv toxins, dendrotoxin-I (*DTX-I*; 100 nM), and rTityustoxin Kα (*rTTSX-Kα*; 10 nM and 50 nM). Note that the outward currents were inhibited significantly by 100 nM DTX-I (*middle traces*) and 50 nM rTTSX-Kα (*lower traces*). In contrast, 10 nM rTTSX-Kα had no effect (see text).

DISCUSSION

Summary of main findings

The results of this study provide the first detailed characterization of the time- and voltage-dependent properties, and the dependence on $[K^+]_o$ of the major K^+ current(s), in freshly isolated rat ventricular fibroblasts. These biophysical and pharmacological results show that rat ventricular fibroblasts express a slowly activating and slowly inactivating K^+ current, which appears to exhibit C-type inactivation. These recordings were made with whole-cell voltage clamp methods applied to fibroblasts isolated enzymatically after Langendorff perfusion of adult rat hearts. The mean value of the resting membrane potential in these rat ventricular fibroblasts was ~−60 mV in physiological $[K^+]_o$ levels (5 mM), and no regenerative responses could be elicited (cf. Chilton et al., 2005).

Biophysical and pharmacological properties of K^+ currents in ventricular fibroblasts

The reversal potential of the tail currents due to deactivation of the outward currents was very close to the calculated K^+ equilibrium potential in each of four different $[K^+]_o$ solutions (Fig. 2). These results demonstrate that this current is highly selective for K^+. In addition, the envelope of tail currents experiments (Fig. 3) suggest that the time- and voltage-dependent K^+ current in cardiac fibroblasts arises from a single component of K^+ conductance.

In all fibroblasts studied, the time- and voltage-dependent K^+ current in cardiac fibroblasts showed slow inactivation with C-type characteristics (Figs. 6–8). Thus, rat ventricular fibroblasts are unlikely to express either Kv1.4 or Kv1.7 or any of the Kv3 or Kv4 families of K^+ channel α-subunits. These transcripts generate fast-inactivating transient K^+ currents (Rasmusson et al., 1998; Coetzee et al., 1999). At present, K^+ currents that exhibit slow-inactivating ''delayed rectifier'' properties, including the Kv1 (but not Kv1.4 and 1.7) and/or Kv2 families (Nerbonne, 1998; Rasmusson et al.,

1998) are considered to be more plausible candidates for the molecular correlates of the K^+ current(s) in cardiac fibroblasts. In agreement with this, DTX-I (100 nM) partially blocked this time- and voltage-dependent K^+ current. The K^+ currents in ventricular fibroblasts were also inhibited by application of 50 nM (but not 10 nM) rTTSX-Kα (Fig. 9). DTX-I is a quite selective blocker for Kv1.1, 1.2, 1.3, and 1.6 (Brew and Forsythe, 1995; Coetzee et al., 1999) and rTTSX-Kα has been reported to block Kv1.3 (Rodrigues et al., 2003) and Kv1.2 with high affinity (ranging from 0.1 to 100 nM) (Ishikawa et al., 2003; Werkman et al., 1993).

The K^+ currents in rat cardiac fibroblasts turned on with a time constant of 20 ms at membrane potentials of +50 mV (in 5 mM $[K^+]_o$). This value of τ for activation is similar to results from cells transfected with Kv1.2 (Hart et al., 1993; Shen et al., 2004) and is similar to the time constant values obtained from cells transfected with Kv1.1, 1.3, 1.5, and 1.6,. These Kv subfamilies are also known to be responsible for slow-inactivating outward K^+ currents (Coetzee et al., 1999; Fedida and Hesketh, 2001), having activation time constants of ~10 ms at membrane potentials near +40 mV (Smart et al., 1997; D'Adamo et al., 1998; Coetzee et al., 1999; Kurata et al., 2001; Watanabe et al., 2003). In summary, the overall biophysical and pharmacological properties of the time- and voltage-dependent K^+ currents in fibroblasts suggest that they may be generated by channels consisting of subunits in the Kv 1.*x* family (cf. Coetzee et al., 1999).

$[K^+]_o$ dependence of ventricular fibroblast K^+ currents

Figs. 4–7 demonstrate that a number of important electrophysiological properties of the voltage-dependent K^+ currents in fibroblasts are strongly modulated by $[K^+]_o$. The half-maximal inactivation of the voltage-dependent K^+ current shifts in the hyperpolarizing direction with increasing $[K^+]_o$ from ~−24 mV in 5 mM to −36 mV in 100 mM $[K^+]_o$ (Fig. 4). This effect of $[K^+]_o$ on the half-maximal inactivation suggests that $[K^+]_o$ can modulate the inactivation states of the voltage-dependent K^+ channels (Kurata et al., 2001). The activation kinetics of the K^+ current in cardiac fibroblasts are significantly faster in 100 mM $[K^+]_o$ than in 5 mM $[K^+]_o$ (Fig. 5). It has been reported previously that application of high $[K^+]_o$ solution during a long depolarization pulse can activate delayed rectifier K^+ current in *Xenopus* axon (Safronov and Vogel, 1995). These findings have been interpreted in terms of an interaction of extracellular K^+ with the inactivated channels, leading to their opening. As shown in Figs. 6 and 7, increasing $[K^+]_o$ slowed the inactivation kinetics. The recovery from inactivation slowed with decreasing $[K^+]_o$. These characteristics, namely that $[K^+]_o$ strongly modulates both rate of inactivation and recovery from inactivation of this outward current, are consistent with known properties of C-type inactivation (Levy and Deutsch, 1996; Rasmusson et al., 1998; Fedida and Hesketh, 2001). These observations lead to the speculation that K^+ channels in cardiac fibroblasts may exhibit a ''foot in the door'' inactivation mechanism (Lopez-Barneo et al., 1993) according to which K^+, as well as other monovalent cations, can occupy site(s) in the external mouth of the K^+ channel, and thus can prevent development of C-type inactivation. As shown in Fig. 8, the K^+ currents in freshly isolated fibroblasts were sensitive to extracellular TEA (30 mM) and the TEA-blocked K^+ channels exhibited enhanced, very slow inactivation (Fig. 8). In summary, our results show that in cardiac fibroblasts, 1), altering $[K^+]_o$ and 2), applying extracellular TEA can modulate the K^+ current activation/inactivation and that these changes are similar to effects reported from earlier studies (Grissmer and Cahalan, 1989; Choi et al., 1991; Baukrowitz and Yellen, 1995; Grigoriev et al., 1999; Fedida and Hesketh, 2001).

Possible functional roles of fibroblast K^+ currents

Having identified the major time- and voltage-dependent K^+ current(s) expressed in acutely isolated cardiac fibroblasts, it is useful to consider their possible electrophysiological roles. This is particularly interesting in view of recent demonstrations of intercellular coupling between fibroblasts, and also between fibroblasts and adjacent ventricular myocytes (Rook et al., 1992; Gaudesius et al., 2003; Camelliti et al., 2004; Goldsmith et al., 2004). The very small size of the fibroblast results in individual cells having a capacitance of only ~5 pF. In the case of the rat ventricular myocyte, which has a capacitance for ~100–110 pF, resistive coupling to some 3–9 fibroblasts would result in what may appear to be an insignificant increase in total capacitance. However, particularly in the setting of a reduced Na^+ current in the myocyte, e.g., the so-called slow response in mammalian heart, this extra capacitance due to fibroblast may alter myocyte excitability. In rat and mouse myocytes, even relatively small changes in rate of rise of the action potential can translate into a significant change in the waveform of early repolarization, and hence can modulate excitation-contraction coupling (Bouchard et al., 1995; Sah et al., 2001, 2003; Libbus et al., 2004). In addition, the action potential in the ventricular myocytes (which precedes each heartbeat) is expected to result in an electrotonic depolarization of the resistively coupled fibroblasts. This may constitute a signal for excitation-secretion coupling in the short-term, and/or for calcium-dependent gene programming in the medium- to longer term. In the mammal ventricle, the consequences of both resistive coupling to fibroblasts and active time and voltage conductances expressed within fibroblasts would be expected to be much more pronounced. In this setting, the relatively long plateau characteristic of the ventricular action potential in all mammals, and the fact that the plateau of the action potential represents a region of relatively high resistance (maintained by very small net currents) would

be expected to augment the effects on action potential waveform of any added capacitance or other electrotonic influences.

In the case of the cardiac fibroblasts, the sensitivity of intrinsic K^+ currents to changes in $[K^+]_o$ may also be important in ventricular function. Early in acute ischemia, $[K^+]_o$ accumulation may cause changes in excitability, conduction, and the refractory period in mammalian myocardium (Fozzard and Makielski, 1985). A number of different animal models of cardiac ischemia show a progressive rise in $[K^+]_o$ over the first few minutes of ischemia. Apparently $[K^+]_o$ can reach levels of 10–15 mM in the ventricular myocardium. The values of half-maximal steady-state inactivation in 10 mM $[K^+]_o$, which we have measured (Fig. 4), suggest that voltage-dependent K^+ channels are still active, even if the reversal potentials (E_m) are shifted in the depolarizing direction by increasing $[K^+]_o$ by 10 mM. In addition, increasing $[K^+]_o$ can enhance activation of these K^+ currents and slow their inactivation. A number of features of our results therefore suggest that functional properties of the voltage-dependent K^+ channels in cardiac fibroblasts may be important during $[K^+]_o$ changes, e.g., acute ischemia.

In summary, our results provide evidence for the significant expression of a time- and voltage-gated K^+ current(s) in rat ventricular fibroblasts. This novel finding and the recent demonstration of resistive coupling between fibroblasts and myocytes need to be considered in the context of the endocrine or paracrine function of the cardiac fibroblast (under both physiological and pathophysiological circumstances). Ongoing experimental work is aimed at molecular identification of the family of K^+ channel α–subunits, which are responsible for the K^+ conductance we have identified. Studies of excitation-secretion coupling in the fibroblast under both physiological and pathophysiological conditions are also of immediate interest.

This study was supported by operating funds from the Canadian Institutes for Health Research and the Heart and Stroke Foundation of Alberta and the Northwest Territories (HSFA). W. Giles held a Chair sponsored by HSFA, and L. Chilton received a fellowship from the Alberta Heritage Foundation for Medical Research and HSFA.

REFERENCES

Attwell, D., D. Eisner, and I. Cohen. 1979. Voltage clamp and tracer flux data: effects of a restricted extra-cellular space. *Q. Rev. Biophys.* 12:213–261.

Barry, P. H. 1994. JPCalc, a software package for calculating liquid junction potential corrections in patch-clamp, intracellular, epithelial and bilayer measurements and for correction junction potential measurements. *J. Neurosci. Methods.* 51:107–116.

Baukrowitz, T., and G. Yellen. 1995. Modulation of K^+ current by frequency and external $[K^+]$: a tale of two inactivation mechanisms. *Neuron.* 15:951–960.

Bouchard, R. A., R. B. Clark, and W. R. Giles. 1995. Effects of action potential duration on excitation-contraction coupling in rat ventricular myocytes. Action potential voltage-clamp measurements. *Circ. Res.* 76:790–801.

Brew, H. M., and I. D. Forsythe. 1995. Two voltage-dependent K^+ conductances with complementary functions in postsynaptic integration at a central auditory synapse. *J. Neurosci.* 15:8011–8022.

Camelliti, P., C. R. Green, I. LeGrice, and P. Kohl. 2004. Fibroblast network in rabbit sinoatrial node: structural and functional identification of homogeneous and heterogeneous cell coupling. *Circ. Res.* 94:828–835.

Chilton, L., E. George, D. MacCannell, I. M. C. Dixon, R. B. Clark, and W. R. Giles. 2003a. Elevated $[K^+]_o$ enhances cultured adult rat cardiac myofibroblast contraction. *J. Physiol. (Lond.).* 551:35a. (Abstr.)

Chilton, L., G. Kargacin, I. Dixon, R. B. Clark, and W. R. Giles. 2003b. An inwardly rectifying K^+ current modulates membrane potential in cultured rat cardiac fibroblasts. *Biophys. J.* 84:225a.

Chilton, L., S. Ohya, D. Freed, E. George, V. Drobic, Y. Shibukawa, K. A. MacCannell, Y. Imaizumi, R. B. Clark, I. M. C. Dixon, and W. R. Giles. 2005. K^+ currents regulate the resting membrane potential, proliferation, and contractile responses in ventricular fibroblasts and myofibroblasts. *Am. J. Physiol. Heart Circ. Physiol.* 288:H2931–H2939.

Choi, K. L., R. W. Aldrich, and G. Yellen. 1991. Tetraethylammonium blockade distinguishes two inactivation mechanisms in voltage-activated K^+ channels. *Proc. Natl. Acad. Sci. USA.* 88:5092–5095.

Coetzee, W. A., Y. Amarillo, J. Chiu, A. Chow, D. Lau, T. McCormack, H. Moreno, M. S. Nadal, A. Ozaita, D. Pountney, M. Saganich, E. Vega-Saenz de Miera, and B. Rudy. 1999. Molecular diversity of K+ channels. *Ann. N. Y. Acad. Sci.* 868:233–285.

D'Adamo, M. C., Z. Liu, J. P. Adelman, J. Maylie, and M. Pessia. 1998. Episodic ataxia type-1 mutations in the hKv1.1 cytoplasmic pore region alter the gating properties of the channel. *EMBO J.* 17:1200–1207.

D'Armiento, J. 2002. Matrix metalloproteinase disruption of the extracellular matrix and cardiac dysfunction. *Trends Cardiovasc. Med.* 12:97–101.

Eghbali, M., M. J. Czaja, M. Zeydel, F. R. Weiner, M. A. Zern, S. Seifter, and O. O. Blumenfeld. 1988. Collagen chain mRNAs in isolated heart cells from young and adult rats. *J. Mol. Cell. Cardiol.* 20:267–276.

Fedida, D., and J. C. Hesketh. 2001. Gating of voltage-dependent potassium channels. *Prog. Biophys. Mol. Biol.* 75:165–199.

Fozzard, H. A., and J. C. Makielski. 1985. The electrophysiology of acute myocardial ischemia. *Annu. Rev. Med.* 36:275–284.

Gaudesius, G., M. Miragoli, S. P. Thomas, and S. Rohr. 2003. Coupling of cardiac electrical activity over extended distances by fibroblasts of cardiac origin. *Circ. Res.* 93:421–428.

Goldsmith, E. C., A. Hoffman, M. O. Morales, J. D. Potts, R. L. Price, A. McFadden, M. Rice, and T. K. Borg. 2004. Organization of fibroblasts in the heart. *Dev. Dyn.* 230:787–794.

Grigoriev, N. G., J. D. Spafford, and A. N. Spencer. 1999. Modulation of jellyfish potassium channels by external potassium ions. *J. Neurophysiol.* 82:1728–1739.

Grissmer, S., and M. Cahalan. 1989. TEA prevents inactivation while blocking open K^+ channels in human T lymphocytes. *Biophys. J.* 55: 203–206.

Hart, P. J., K. E. Overturf, S. N. Russell, A. Carl, J. R. Hume, K. M. Sanders, and B. Horowitz. 1993. Cloning and expression of a Kv1.2 class delayed rectifier K^+ channel from canine colonic smooth muscle. *Proc. Natl. Acad. Sci. USA.* 90:9659–9663.

Hille, B. 2001. Ion Channels of Excitable Membranes, 3rd ed. Sinauer Associates, Sunderland, MA.

Hodgkin, A. L., and A. F. Huxley. 1952. A quantative description of membrane current and its application to conduction and excitation in nerve. *J. Physiol. (Lond.).* 117:500–544.

Hoshi, T., W. N. Zagotta, and R. W. Aldrich. 1990. Biophysical and molecular mechanisms of Shaker potassium channel inactivation. *Science.* 250:533–538.

Hoshi, T., W. N. Zagotta, and R. W. Aldrich. 1991. Two types of inactivation in Shaker K^+ channels: effects of alterations in the carboxy terminal region. *Neuron*. 7:547–556.

Ishikawa, T., Y. Nakamura, N. Saitoh, W. B. Li, S. Iwasaki, and T. Takahashi. 2003. Distinct roles of Kv1 and Kv3 potassium channels at the calyx of Held presynaptic terminal. *J. Neurosci.* 23:10445–10453.

Kamkin, A., I. Kiseleva, and G. Isenberg. 2003. Activation and inactivation of a non-selective cation conductance by local mechanical deformation of acutely isolated cardiac fibroblasts. *Cardiovasc. Res.* 57:793–803.

Kohl, P., A. G. Kamkin, I. S. Kiseleva, and D. Noble. 1994. Mechanosensitive fibroblasts in the sino-atrial node region of rat heart: interaction with cardiomyocytes and possible role. *Exp. Physiol.* 79:943–956.

Kurata, H. T., G. S. Soon, and D. Fedida. 2001. Altered state dependence of C-type inactivation in the long and short forms of human Kv1.5. *J. Gen. Physiol.* 118:315–332.

Levy, D. I., and C. Deutsch. 1996. Recovery from C-type inactivation is modulated by extracellular potassium. *Biophys. J.* 70:798–805.

Libbus, I., X. Wan, and D. S. Rosenbaum. 2004. Electrotonic load triggers remodeling of repolarizing current I_{to} in ventricle. *Am. J. Physiol. Heart Circ. Physiol.* 286:H1901–H1909.

Long, C. S., and R. D. Brown. 2002. The cardiac fibroblast, another therapeutic target for mending the broken heart? *J. Mol. Cell. Cardiol.* 34:1273–1278.

Lopez-Barneo, J., T. Hoshi, S. H. Heinemann, and R. W. Aldrich. 1993. Effects of external cations and mutations in the pore region on C-type inactivation of Shaker potassium channels. *Receptors Channels.* 1: 61–71.

Nerbonne, J. M. 1998. Regulation of voltage-gated K^+ channel expression in the developing mammalian myocardium. *J. Neurobiol.* 37:37–59.

Noble, D., and R. W. Tsien. 1969. Outward membrane currents activated in the plateau range of potentials in cardiac Purkinje fibres. *J. Physiol. (Lond.).* 200:205–231.

Rasmusson, R. L., M. J. Morales, S. Wang, S. Liu, D. L. Campbell, M. V. Brahmajothi, and H. C. Strauss. 1998. Inactivation of voltage-gated cardiac K^+ channels. *Circ. Res.* 82:739–750.

Rodrigues, A. R., E. C. Arantes, F. Monje, W. Stuhmer, and W. A. Varanda. 2003. Tityustoxin-K(alpha) blockade of the voltage-gated potassium channel Kv1.3. *Br. J. Pharmacol.* 139:1180–1186.

Rook, M. B., A. C. van Ginneken, B. de Jonge, A. el Aoumari, D. Gros, and H. J. Jongsma. 1992. Differences in gap junction channels between cardiac myocytes, fibroblasts, and heterologous pairs. *Am. J. Physiol.* 263:C959–C977.

Safronov, B. V., and W. Vogel. 1995. Modulation of delayed rectifier K^+ channel activity by external K^+ ions in *Xenopus* axon. *Pflugers Arch.* 430:879–886.

Sah, R., R. J. Ramirez, R. Kaprielian, and P. H. Backx. 2001. Alterations in action potential profile enhance excitation-contraction coupling in rat cardiac myocytes. *J. Physiol. (Lond.).* 533:201–214.

Sah, R., R. J. Ramirez, G. Y. Oudit, D. Gidrewicz, M. G. Triveri, C. Zobel, and P. H. Backx. 2003. Regulation of cardiac excitation-contraction coupling by action potential repolarization: role of the transient outward potassium current (I_{to}). *J. Physiol. (Lond.).* 546:5–18.

Sanguinetti, M. C., and N. K. Jurkiewicz. 1990. Two components of cardiac delayed rectifier K^+ current. Differential sensitivity to block by class III antiarrhythmic agents. *J. Gen. Physiol.* 96:195–215.

Shen, W., S. Hernandez-Lopez, T. Tkatch, J. E. Held, and D. J. Surmeier. 2004. Kv1.2-containing K^+ channels regulate subthreshold excitability of striatal medium spiny neurons. *J. Neurophysiol.* 91:1337–1349.

Shiraishi, I., T. Takamatsu, T. Minamikawa, Z. Onouchi, and S. Fujita. 1992. Quantitative histological analysis of the human sinoatrial node during growth and aging. *Circulation.* 85:2176–2184.

Smart, S. L., M. M. Bosma, and B. L. Tempel. 1997. Identification of the delayed rectifier potassium channel, Kv1.6, in cultured astrocytes. *Glia.* 20:127–134.

Suh, S. H., R. Vennekens, V. G. Manolopoulos, M. Freichel, U. Schweig, J. Prenen, V. Flockerzi, G. Droogmans, and B. Nilius. 1999. Characterisation of explanted endothelial cells from mouse aorta: electrophysiology and Ca^{2+} signalling. *Pflugers Arch.* 38:612–620.

Tomasek, J. J., G. Gabbiani, B. Hinz, C. Chaponnier, and R. A. Brown. 2002. Myofibroblasts and mechano-regulation of connective tissue remodelling. *Nat. Rev. Mol. Cell Biol.* 3:349–363.

Villarreal, F. J., and N. N. Kim. 1998. Regulation of myocardial extracellular matrix components by mechanical and chemical growth factors. *Cardiovasc. Path.* 7:145–151.

Villarreal, F. J., N. N. Kim, G. D. Ungab, M. P. Printz, and W. H. Dillmann. 1993. Identification of functional angiotensin II receptors on rat cardiac fibroblasts. *Circulation.* 88:2849–2861.

Watanabe, I., H. G. Wang, J. Sutachan, J. Zhu, E. Recio Pinto, and W. B. Thornhill. 2003. Glycosylation affects rat Kv1.1 potassium channel gating by a combined surface potential and cooperative subunit interaction mechanism. *J. Physiol. (Lond.).* 550:51–66.

Werkman, T. R., T. A. Gustafson, R. S. Rogowski, M. P. Blaustein, and M. A. Rogawski. 1993. Tityustoxin-K alpha, a structurally novel and highly potent K^+ channel peptide toxin, interacts with the alpha-dendrotoxin binding site on the cloned Kv1.2 K^+ channel. *Mol. Pharmacol.* 44:430–436.

Yasui, K., T. Anno, K. Kamiya, M. R. Boyett, I. Kodama, and J. Toyama. 1993. Contribution of potassium accumulation in narrow extracellular spaces to the genesis of nicorandil-induced large inward tail current in guinea-pig ventricular cells. *Pflugers Arch.* 422:371–379.

Zagotta, W. N., T. Hoshi, and R. W. Aldrich. 1990. Restoration of inactivation in mutants of Shaker potassium channels by a peptide derived from ShB. *Science.* 250:568–571.